SUPPLEMENTARY INFORMATION FOR: MAXIMIZING TANDEM SOLAR CELL POWER EXTRACTION USING A THREE-TERMINAL DESIGN

Emily L. Warren,*[,a] Michael G. Deceglie,[a] Michael Reinäcker,[b] Robby Peibst,[b] Adele C. Tamboli, [a]and Paul Stradins[a]

[a] National Renewable Energy Lab, Golden, CO, USA; E-mail: emily.warren@nrel.gov [b] Institute for Solar Energy Research Hamelin, Emmerthal, Germany

I. DETAILS OF ELECTRICAL DEVICE SIMULATION

The geometry of the simulated device consists of an n-type Si substrate with interdigitated back polysilicon on oxide (POLO) contacts consisting of an interfacial SiO_2 and heavily doped poly-Si of both polarities. The poly-Si regions are contacted with Al through smaller area openings within a dielectric layer (shown in Fig. 2a of main text). The entire front surface of the cell was coated with an n-type POLO contact and defined as a uniform contact to simulate the performance of a transparent conductive adhesive (TCA) layer. For simplicity, the poly-Si layers are electrically defined as separate c-Si regions with different doping densities, and any photogeneration in these layers is ignored.[9]

The passivated contact structure was modeled for n-type contacts using a thin tunneling SiO_2 layer, as has been previously demonstrated,[10,11] and by specifying the electron and hole recombination velocities at the c-Si/poly-Si interface.[4] Having a well-passivated interface at the front of the cell is critical to achieve high efficiency devices. Two terminal (2T) simulations of a similar device without any front passivation (assuming ohmic contact), resulted in severely degraded cell performance in both front-back (FB) and IBC mode.[12] In POLO experimental devices, dopants from the poly-Si diffuse into the bulk wafer through the oxide passivation layer. This phenomena was simulated using Gaussian doping profiles to approximate the maximum concentration and depth of in-diffusion. Table I lists the geometric and doping parameters used to simulate the Si device.

To accurately model Si solar cell behavior, physical models were chosen based on the recommendations of Altermatt and prior simulation of passivated contact Si devices.[3,4,10] Recombination at all semiconductor/metal contacts was defined by specifying electron and hole recombination velocities. Recombination at semiconductor/semiconductor or semiconductor/dielectric surfaces was accounted for using a surface Shockley-Read-Hall model.[1] The models and model inputs used for the simulation are listed in Table II.

To enable comparison of different operation modes, simulations in 2T and 4T mode were carried out for comparison to the 3T device. Although cells with different numbers of terminals would be optimized slightly differently with regards to doping profiles, contact geometry, etc., in this work simulations of different cell configurations all used the same device geometry and doping to enable direct comparison of different operation modes. In practice, a 2T Si solar cell with FB contacts can be made with a blanket emitter back contact and not interdigitated back contacts. Simulations comparing a device with a full-back emitter and an optimized selective emitter such as that used in a POLO device only showed a minor difference in device performance. 4T devices were simulated using the IBC contacts of the Si cell, because the TCA interconnection that is optically simulated does not enable the lateral current extraction that is needed. Note that for a 4T tandem device, an additional grid would be needed to extract current from the back of the top cell, that would add additional shading loss to the bottom cell, so the 4T results presented for comparison are potentially a slight over-estimate of the achievable 4T tandem performance.

TABLE I. Geometry of Si cell

Parameter	Value
Cell thickness	160 μm
Unit cell width	365 μm
Bulk doping (P)	1x10^{15} cm^{-3}
Bulk lifetime	10 ms
poly-Si thickness	20 nm
poly-Si doping	1.5x10^{19} cm^{-3}
Front n-contact parameters	
Contact width	365 μm
Tunnel oxide thickness	1.5 nm
P In-diffusion depth	300 nm
P In-diffusion peak	1x10^{19} cm^{-3}
Back n-contact parameters	
Contact width	100 μm
Tunnel oxide thickness	1.5 nm
P In-diffusion depth	800 nm
P In-diffusion peak	1x10^{20} cm^{-3}
Back emitter contact parameters	
Contact width	250 μm
B In-diffusion depth	500 nm
B In-diffusion peak	5x10^{19} cm^{-3}

TABLE II. Device parameters for Si cell

Parameter	Value
Temperature	300 K
Statistics	Fermi-Dirac
Free Carrier Mobility	Phillips Unified
BandGapNarrowing	Schenk
Auger Recombination	Richter
Tunneling model	Nonlocal tunneling
Tunneling effective mass ($m_{e,h}$)	0.4
Region-specific recombination parameters	
SRV at c-Si/SiO_2 interface	10^3 cm/s
SRV at c-Si/SiN_x interface	50 cm/s
SRV at c-Si/poly-Si_x interface	100 cm/s
SRV at metal contacts	$v_n = v_p = 10^7$ cm/s

II. DETAILS OF OPTICAL DEVICE SIMULATIONS

Vastly different length scales are needed to capture the electrical and optical performance of an IBC device, so it common practice in the TCAD modeling of solar cells to first calculate an optical generation profile and then use this profile to solve the device physics of the cell.[1] This enables the optical generation profile to guide the meshing of the device area, so that regions of high optical absorption are meshed more densely, which enhances the efficiency of convergence of the device physics model. All optical generation profiles were

TABLE III. Device parameters for Si cell

Air Mass	APE (eV)	Total Power (mW cm^{-2})
AM 1	1.84	93.09
AM 1.5	1.80	100.45
AM 2	1.78	86.81
AM 3	1.74	67.85
AM 4	1.71	55.78
AM 5	1.68	47.32

created PV Lighthouse's module ray-tracing software.[2] For simulations under standard conditions, the ASTM G-173-03 spectrum was used. For varying the incident spectra on the cell, SMARTS 2.9.5 was used to calculate spectra with varying air mass (AM1 to AM5).[7] Table III lists the average photon energy (APE) of each spectra calculated from 280 nm to 1200 nm, and the total spectral power, calculated across the entire spectrum, including sub-bandgap wavelengths. Note that for consistency with SMARTS-generated spectra, the total spectral power used for AM1.5G is 100.45 mW cm^{-2}, which is slightly different than the standard 100 mW cm^{-2} often used for solar cell efficiency calculations.

Each spectrum was then used as an input into a module Monte Carlo ray tracer, which was used to create a generation profile. The full device stack simulated is shown in Fig 1a. The front of the Si devices was assumed to be planar, but the backs were randomly textured. A uniform 1% shading loss was included to account for absorption in the TCA material, based on experimentally demonstrated performance.[6] Sensitivity analyses were performed to optimize thicknesses of TCO and ARC layers, and to verify that the sensitivity to the spacing between the top and bottom cell does not have a large impact on the generation profile of the Si subcell. Luminescent coupling between the subcells was assumed to be negligible, and losses due to fingers, shading, or differences in reflectivity of metallized regions of the back contact were not considered.

The simulated EQE for a GaInP/Si tandem is shown in Fig 1b, along with the certified EQE measured for the champion GaInP/Si 4T tandem reported by Essig et al.[5] The Si cell used for the experiments was a textured heterojunction device with ITO and a-Si at the front of the cell, and mounted behind a glass slide with epoxy. The front coatings are similar to the front surface of the 3T POLO devices, but the simulated optical properties of the ITO layers and poly-Si at the front of the Si cell are different than those used in the experimental measurement. The simulated EQE does not include the optical losses from grid fingers, and while the experimental device has grid fingers at the front and in between the two subcells, the EQE data was collected between fingers. While there are several differences between the structure simulated and the experimental cell, the comparison demonstrates that the simulated generation is a reasonable estimate of what might be attainable in an optimized TCA interconnected cell.

III. CALCULATING POWER AND EFFICIENCY FOR SI SUB-CIRCUIT AND TANDEM DEVICES

The output of the TCAD simulations provides the potential and current of each contact. To accurately calculate the power and efficiency of the device, it is important to accurately define the current densities and voltages, as the raw outputs of the simulation are not scaled appropriately. Equations 1 and 2 were used to define V_{IBC} and V_{FB}, which can then be used to calculate the power of the sub-circuit. The following equations summarize how the power of each sub-circuit of the 3T Si are calculated from simulation data:

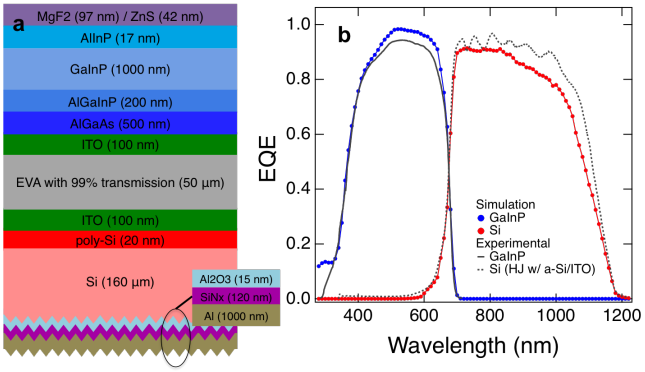

FIG. 1. (a) Simulated stack for creating generation profiles and (b) comparison of simulated and experimental EQE for mechanically integrated GaInP/Si tandem cells.

$$V_{IBC} = V_{p,back} - V_{n,back} \quad (1)$$
$$V_{FB} = V_{p,back} - V_{n,front} \quad (2)$$
$$P_{Si,IBC} = I_{IBC} * V_{IBC} \quad (3)$$
$$P_{Si,FB} = I_{IBC} * V_{FB} \quad (4)$$
$$P_{Si,Tot} = P_{Si,IBC} + P_{Si,FB} \quad (5)$$

The following equations summarize how the total power of the tandem devices are calculated for 2T, 3T, and 4T interconnection configurations.

$$P_{2TT} = I_{FB,tandem} * (V_{IIIV} + V_{Si,FB}) \quad (6)$$
$$P_{4TT} = (I_{IIIV} * V_{IIIV}) + (I_{Si,IBC} * V_{Si,IBC}) \quad (7)$$
$$P_{3TT} = I_{FB,tandem} * (V_{IIIV} + V_{Si,FB}) + (I_{IBC} * V_{IBC}) \quad (8)$$

IV. EXPERIMENTAL 3T MEASUREMENTS

To confirm our simulation results, we have compared our modeled performance to experimental measurements of 3T POLO Si cells measured as 1J devices (i.e. without a top cell).[8] Experiments were carried out under non-standard illumination conditions where the incident power of the light on the back of the cell was adjusted to give a short-circuit current density of 10 mA for a 1 cm^2 device. Figure 2 shows that the performance in FB and IBC mode is nearly identical which supports the simulated results of the same device structure.

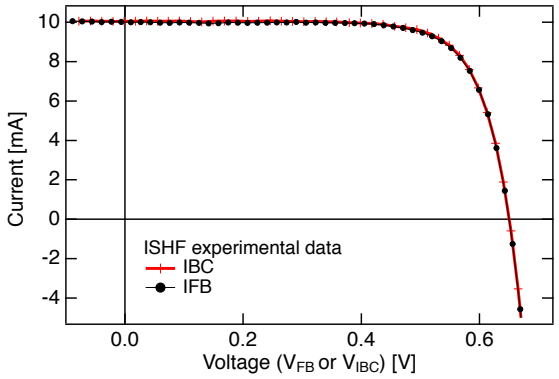

FIG. 2. Experimental I-V data for a 3T Si POLO cell measured in FB and IBC mode. Illumination was provided from an uncalibrated source, adjusted to give a current of 10 mA for a 1 cm^2 device.

V. REFERENCES

[1] Optimization of Rear Contact Design in Monocrystalline Silicon Solar-Cell Using 3D TCAD Simulations. Technical report, 2011.

[2] https://www.pvlighthouse.com.au, last accessed Nov 5, 2017.

[3] Pietro P. Altermatt. Models for numerical device simulations of crystalline silicon solar cells - A review. Journal of Computational Electronics, 10(3):314–330, 2011.

[4] Chia-Wei Chen, Martin Hermle, Jan Benick, Yuguo Tao, Young-Woo Ok, Ajay Upadhyaya, Andrew M. Tam, and Ajeet Rohatgi. Modeling the potential of screen printed front junction CZ silicon solar cell with tunnel oxide passivated back contact. Progress in Photovoltaics: Research and Applications, 25(1):49–57, 2017. PIP-16-070.R1.

[5] Stephanie Essig, Christophe Allebé, Timothy Remo, John F. Geisz, Myles A. Steiner, Kelsey Horowitz, Loris Barraud, J. Scott Ward, Manuel Schnabel, Antoine Descoeudres, David L. Young, Michael Woodhouse, Matthieu Despeisse, Christophe Ballif, and Adele Tamboli. Raising the one-sun conversion efficiency of III–V/Si solar cells to 32.8% for two junctions and 35.9% for three junctions. Nature Energy, 2:17144, 08 2017.

[6] Talysa Klein, Benjamin Lee, Manuel Schnabel, Emily Warren, Paul Stradins, Adele Tamboli, and Maikel F. A. M. van Hest. Transparent conductive adhesives for tandem solar cells using polymer-particle composites. ACS Applied Materials & Interfaces, 10(9):8086–8091, 2018.

[7] D. R. Myers and C. A. Gueymard. Description and Availability of the SMARTS Spectral Model for Photovoltaic Applications. Proc. SPIE, 5520:1–12, August 2004.

[8] M. Rienäcker, E. L. Warren, M. Schabel, H. Schulte-Huxel, A. Merkle, S. Kajari-Schöder, R. Niepelt, R. Brendel, P. Stradins, A. Tamboli, and R. Peibst. Maximum power extraction enabled by monolithic tandems using interdigitated back contact bottom cells with three terminals. In Prep., 2018.

[9] Udo Römer, Robby Peibst, Tobias Ohrdes, Bianca Lim, Jan Krügener, Eberhard Bugiel, Tobias Wietler, and Rolf Brendel. Solar Energy Materials & Solar Cells Recombination behavior and contact resistance of n and p poly-crystalline Si / monocrystalline Si junctions. Solar Energy Materials and Solar Cells, 131:85–91, 2014.

[10] H Steinkemper, F Feldmann, M Bivour, and M Hermle. Numerical Simulation of Carrier-Selective Electron Contacts Featuring Tunnel Oxides. IEEE Journal of Photovoltaics, 5(5):1348–1356, 2015.

[11] H Steinkemper, F Feldmann, M Bivour, and M Hermle. Theoretical Investigation of Carrier-selective Contacts Featuring Tunnel Oxides by Means of Numerical Device Simulation. Energy Procedia, 77(5):195–201, 2015.

[12] Emily L Warren, Michael G Deceglie, Paul Stradins, and Adele C Tamboli. Modeling Three-Terminal III-V/Si Tandem Solar Cells. In Proceedings of 44th PVSC. IEEE, 2017.